J Appl Electrochem (2007) 37:669–674
DOI 10.1007/s10800-007-9299-z

ORIGINAL PAPER

Current efficiency and kinetics of cobalt electrodeposition in acid chloride solutions. Part I: The influence of current density, pH and temperature

O. E. Kongstein · G. M. Haarberg · J. Thonstad

Received: 8 February 2005 / Accepted: 22 January 2007 / Published online: 24 March 2007

Abstract In the electrodeposition of cobalt in chloride electrolytes the evolution of hydrogen is a parasitic reaction. On a rotating platinum disc electrode the current efficiency was calculated as the charge used for anodic dissolution of cobalt at a potential where no other reactions were taking place, divided by the total cathodic charge used for cobalt deposition. The results show that the current efficiency could be measured accurately in this way. In part I the current efficiency and deposition potential are studied as a function of current density and pH. The results show an increase in current efficiency with increasing current density, pH and temperature. The results also indicate a change in the reaction mechanism for electrodeposition when the pH is changed.

Keywords Cobalt · Current-efficiency · Electrodeposition · Overpotential

1 Introduction

Industrial electrowinning of cobalt is usually carried out in sulphate electrolytes [1]. Only the Falconbridge electrowinning plant in Norway and the Sumitomo Company in Japan are operating in chloride electrolytes [2–4]. The advantages of using chloride electrolytes compared with sulphate can be summarised as higher electrical conductivity in the electrolyte, lower overpotential for deposition of cobalt and lower anodic overpotentials, higher cathodic current efficiency and easier and more specific nickel–cobalt separation by solvent extraction. The disadvantage of using chloride electrolyte is the fact that the anode gas must be collected, and according to Fujimori et al. [2], the stress induced during the deposition of cobalt metal is higher in chloride solutions. The purpose of the present work was to carry out a parametric study of cobalt electrowinning in order to enhance the understanding of factors of importance for the industrial process.

2 Experimental

The electrolyte used in the experiments was usually a solution of cobalt chloride containing some sodium chloride and hydrochloric acid. The composition of this electrolyte and the standard experimental conditions are given in Table 1.

Hydrochloric acid and sodium hydroxide were used to adjust the electrolyte pH in the cobalt chloride electrolytes. Current efficiency experiments at constant potential were performed using a rotating platinum disc electrode with diameter 4 mm, with cobalt as counter electrode. The electrode potential was measured vs. a saturated calomel electrode.

An EG&G Princeton Applied Research model 173 potentiostat/galvanostat with a digital coulometer was used. Before the experiments started, the electrolyte was degassed with nitrogen for approximately one hour, to remove dissolved oxygen. During the experiments nitrogen was passed under the cell cover. The time and the electric charge were recorded during the

O. E. Kongstein (✉) · G. M. Haarberg · J. Thonstad
Department of Materials Science and Engineering,
Norwegian University of Science and Technology,
7491 Trondheim, Norway
e-mail: oleko@nt.ntnu.no

Table 1 Standard experimental conditions

Experimental conditions		Electrolyte composition	
		Element	Concentration/M
Deposition charge	0.6 C	Co^{2+}	0.92
Rotation rate	100 r.p.m.	Na^{+}	0.19
pH	1.23 at 60 °C	H^{+}	0.035
Temperature	60 °C	Ni^{2+}	7.8×10^{-4}
Electrolyte volume	0.9×10^{-3} m^3	Fe^{2+}	$<2.1 \times 10^{-7}$
Electrode area	1.26×10^{-5} m^2	Pb^{2+}	4.8×10^{-6}
		Zn^{2+}	$<3.1 \times 10^{-6}$
		Cl^{-}	2.07

experiments. The experiment was stopped when a given amount of charge was reached. The disc electrode was then taken out of the cell and examined visually and any gas bubbles adhering to the surface were removed by blowing air. Subsequently the electrode was reinstalled into the reactor, and the plated cobalt was dissolved anodically at +0.241 V_{SHE}, and the charge passed was recorded again. IR compensation was not used during these experiments; the resistance in the electrolyte was measured with a Radiometer Copenhagen DEA 322 digital electrochemical analyzer and IMT 102 electrochemical interface, and taken into account after the experiments by using the expression: $|E| = |E_{adjusted}| - IR$. An illustration of the current response is given in Fig. 1.

The current efficiency (CE) for cobalt deposition was calculated from Eq. 1.

$$\mathrm{CE} = 100 \cdot \frac{Q^A}{Q^C} \tag{1}$$

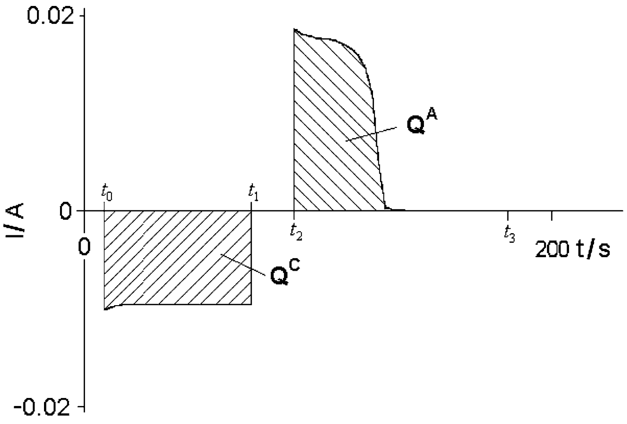

Fig. 1 Plot of current versus time on a rotating platinum disc electrode. The adjusted potential in the time interval t_0 to t_1 was –0.800 V_{SCE} (–0.559 V_{SHE}), and the adjusted potential between t_2 and t_3 was 0.000 V_{SCE} (0.241 V_{SHE})

The symbols used in Eq. 1 are explained in Fig. 1. The partial current density for cobalt deposition was calculated from Eq. 2. The average current density was calculated from the cathodic charge, and the time at cathodic polarization.

$$i_{\mathrm{Co}} = \frac{\mathrm{CE} \cdot i_{\mathrm{ave}}}{100} \tag{2}$$

Under the assumption that all the loss in current efficiency for cobalt deposition was represented by the partial current for hydrogen evolution, the partial current density for this reaction could be calculated from Eq. 3.

$$i_{\mathrm{H}_2} = i_{\mathrm{ave}} - i_{\mathrm{Co}} \tag{3}$$

3 Results and discussion

3.1 Method

3.1.1 *Cathodic charge*

The purpose of these experiments was to assess the amount of cathodic charge needed to determine the current efficiency without any influence from the initial stages of cobalt deposition and hydrogen evolution on the platinum surface. The cathodic charge (time) was varied at a potential of –0.477 V_{SHE}; the rest of the experimental conditions are given in Table 1.

Figure 2 shows that when a very small cathodic charge was applied, the current efficiency was low compared with experiments where larger quantities of charge were passed. At a given potential the current consumed for hydrogen evolution is higher on platinum than on cobalt, and at the start of each experiment the cathode surface was platinum. After a short time the whole surface was covered by cobalt and the hydrogen evolution could only take place on plated cobalt. Above 0.3 C, corresponding to a deposit of 0.72 μm thickness, the current efficiency reached a stable value, where the initial hydrogen evolution on platinum had only a minor effect on the total current efficiency.

3.1.2 *Reproducibility of current efficiency experiments*

The applied potential was –0.477 V_{SHE} and the cathodic charge was 0.6 C; the other experimental conditions are given in Table 1. The experiment was repeated five times and the average current efficiency became 88.9 ± 0.8 within the 95% confidence interval. The nearly constant current efficiency means that

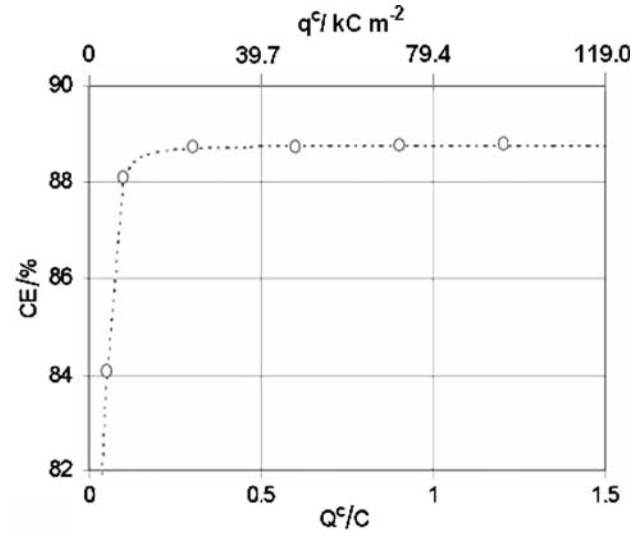

Fig. 2 Current efficiency versus the applied charge and charge density for electrodeposition

cobalt did not spall off the electrode during the experiments.

The main problem in the experiments carried out with the rotating disc electrode was that hydrogen gas bubbles were formed and adhered to the electrode surface. This problem was more pronounced at low current efficiencies. To control this problem the electrode was inspected after each experiment and, if there were many gas pits on the surface, the experiment was repeated.

A binary phase diagram for cobalt and platinum is given by Hultgren et al. [5]; this diagram shows that intermetallics of cobalt and platinum are stable at room temperature. This means that a Co–Pt compound could be formed during electrodeposition. The measured current efficiency for cobalt deposition from the electrolyte in Table 1 at pH 4.37 in the current density range 100–1000 A m^{-2} was above 99.7%. The current efficiencies were slightly below 100%, caused by hydrogen evolution. The Tafel parameters from these experiments are given in Table 2, marked pH 4.37. The results indicate that no Co–Pt compounds were formed that were difficult to dissolve anodically. After the platinum electrode was polished, a few experiments were performed to condition the surface before the real experiments started.

Table 2 Calculated kinetic parameters for deposition of cobalt as a function of pH

pH	b_c/V decade^{-1}	log(i_0/A m^{-2})	log(i/A m^{-2}) at –0.500 V_{SHE}	1–β
4.37	–0.033 ± 0.003	–0.9 ± 0.3	5.6 ± 0.3	0.51 ± 0.05
2.08	–0.067 ± 0.004	–0.6 ± 0.2	2.57 ± 0.05	0.49 ± 0.04
1.58	–0.066 ± 0.007	–0.5 ± 0.3	2.69 ± 0.07	0.5 ± 0.06
1.23	–0.067 ± 0.004	–0.6 ± 0.2	2.56 ± 0.07	0.49 ± 0.03
1.08	–0.067 ± 0.003	–0.6 ± 0.1	2.59 ± 0.03	0.49 ± 0.02

3.2 Influence of pH

The purpose of these experiments was to investigate the influence of pH on the current efficiency and on the overpotential for deposition of cobalt and for hydrogen evolution. The pH was varied at five levels, and the rest of the experimental conditions were as described in Table 1. As an example, Tafel plots obtained at pH 1.23 are given in Fig. 3. Plots of the potential versus the logarithm of the partial current density for cobalt deposition and for hydrogen evolution are given in the figure, and the regression lines calculated by least squares fit are shown.

In order to make sure that any mass transfer limitations of cobalt ion could be ignored, the limiting current was measured. Because of dendritic growth and influence of migration an electrolyte with 0.046 M $CoCl_2$(aq) and 1 M $CaCl_2$ at 60 °C was used. In the experiment the limiting current was found to be 214 A m^{-2} at 100 r.p.m. corresponding to a limiting current density of 4280 A m^{-2} at 0.92 M $CoCl_2$(aq).

Many similar measurements to that presented in Fig. 3 were carried out at different experimental conditions. In the same way as shown in Fig. 3, the Tafel parameters were derived at the other pH values. The results are listed in Table 2, where the error limits are at 95% confidence intervals from the regression lines. The reversible potential for deposition of cobalt used in the calculation of the exchange current density in

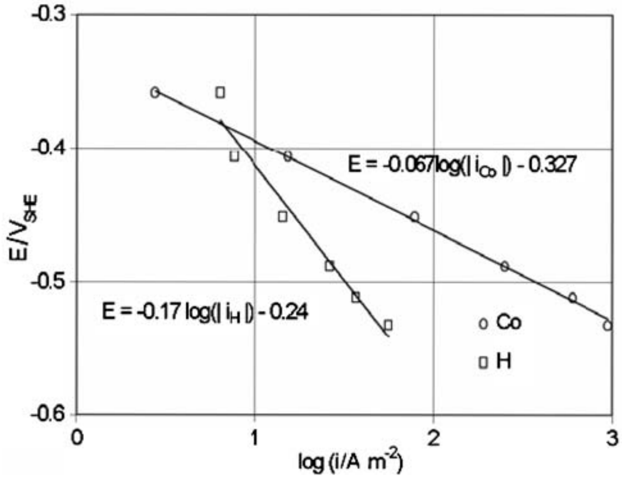

Fig. 3 Tafel plots for cobalt deposition and hydrogen evolution at pH 1.23

Table 2 was –0.288 V_{SHE}. This value was calculated from activity coefficients given by Gmelin [6], and thermodynamic data taken from SI Chemical Data [7].

The values of 1-β listed in Table 2 were calculated from Eq. 5 assuming a two-electron transfer. Table 2 shows that the Tafel slopes and the exchange current densities for cobalt deposition were different at pH 4.37 compared to at pH 1.08 to 2.08. At pH between 1.08 and 2.08 the exchange current densities and the Tafel slopes have the same value, independent of pH. This indicates that the mechanism was not influenced by this change in pH.

The current efficiencies for deposition of cobalt calculated from the same experiments as the Tafel parameters in Table 2 are given in Fig. 4. Many workers have found an increase in current efficiency for cobalt with increasing pH both in chloride electrolytes [8–10] as well as in sulphate electrolytes [11–13]. Figure 4 shows that the current efficiency increased with increasing pH and with increasing current density. The reason for higher current efficiency when the pH was increased was that hydrogen evolution was suppressed at higher pH. The reason for increasing current efficiency with current density was that the Tafel slope for hydrogen evolution is steeper than the Tafel slope for deposition of cobalt, as shown in Fig. 3. In Fig. 4 it seems as if the current efficiency was almost independent of increasing current density at high current densities. This effect arises because the current density is close to an exponential function of the potential, so the increase in potential was minor between the experimental points at high current densities.

The experiment recorded in Fig. 5 was carried out on a stationary electrode with diameter 2 cm, because hydrogen evolution was a serious problem in long term experiments on rotating discs. Initially the pH measured at 60 °C was 4.37, and the rest of the experimental parameters were as given in Table 1. Before the experiment started cobalt was plated on the electrode for approximately one hour at 230 A m^{-2}. During the experiment the potential was kept at –0.409 V_{SHE} and HCl(aq) was added, and the pH at 60 °C and the current were measured point by point. The current density as a function of electrolyte pH is shown in Fig. 5, which shows that the current density was strongly influenced by pH down to about pH 3. This indicates that deposition of cobalt was pH dependent between pH 4.37 and 3. This is in good agreement with the Tafel slopes for electrodeposition of cobalt given in Table 2, where the Tafel slope at pH 4.37 was –0.033 V $decade^{-1}$ and –0.067 V $decade^{-1}$ at pH 2.08, which also indicates a change in the reaction mechanism for electrodeposition with changing pH. From Fig. 5 it can be seen that the current tended to increase at low pH. This effect can be explained by the fact that more current is consumed by hydrogen evolution at lower pH. The same trends as shown in Fig. 5 were also reported by Scoyer and Winand [8] and Louis et al. [9] in chloride electrolytes, and by Feneau and Breckpot [14] in sulphate electrolyte.

Heusler [15, 16] suggested a pH dependent deposition mechanism for cobalt from cobalt perchlorate electrolyte, where cobalt was deposited through the intermediate $CoOH^{+}(aq)$. Cui et al. [17] proposed the same mechanism for chloride electrolytes. Bolzan and Arvìa [18] and Smith and Martell [19] have suggested the following hydrolysis reaction of the cobaltous ion:

$$Co^{2+}(aq) + H_2O \leftrightarrow CoOH^{+}(aq) + H^{+}(aq) \tag{4}$$

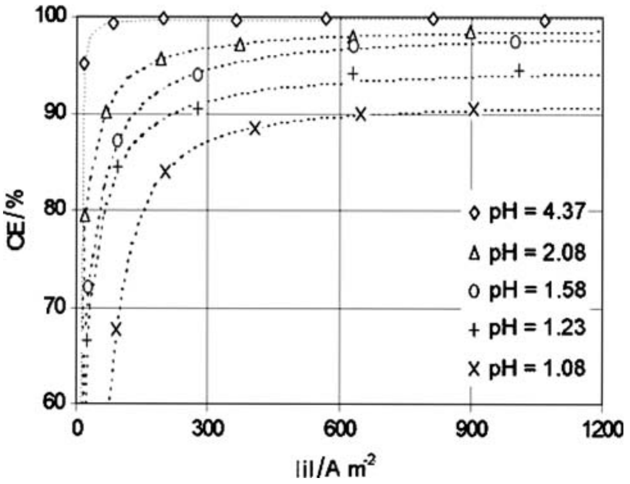

Fig. 4 Current efficiency for cobalt deposition versus current density at different pH values

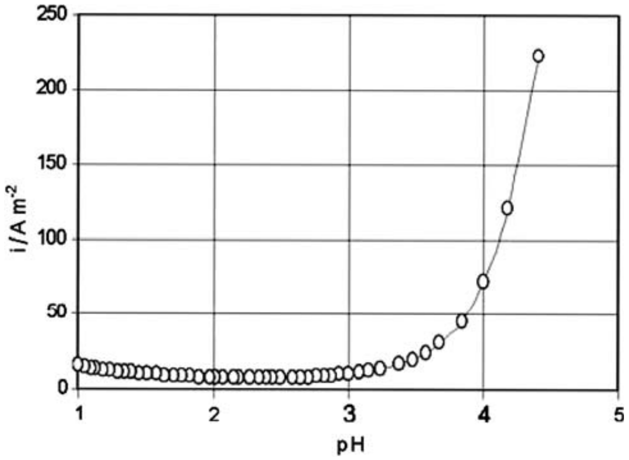

Fig. 5 Average current density versus pH at –0.409 V_{SHE}

For Eq. 4 the expression for the equilibrium constant given by [18] was; $log(Ka) = -3.82 - 1785 \times T^{-1}$. At 25 °C and ionic strength equal to 1, the log(K) value from Eq. 4 is given to be –10.1 in [19], in good agreement with the value from [18]. From the equilibrium in Eq. 4 it can be seen that the value of $a_{CoOH^+}(aq)$ will decrease with increasing a_{H^+} (aq), so that $a_{CoOH^+(aq)}$ becomes very low at low pH. On this basis it is probable that cobalt deposition is pH dependent at high pH and independent at low pH.

3.3 Influence of temperature

In these experiments the temperature was varied at four levels; the electrolyte composition is given in Table 1. The calculated Tafel parameters for cobalt deposition by varying temperature are given in Table 3. The Tafel slope became steeper at high temperatures; this effect is in agreement with Eq. 5:

$$b^C = -\frac{RT\ln(10)}{(1-\beta)nF} \tag{5}$$

Table 3 also shows that the exchange current density for electrodeposition was strongly dependent on temperature, while the value of (1-β) did not vary. The current density at –0.500 V_{SHE} in Table 3 increases with increasing temperature, indicating a reduced overpotential for cobalt deposition. According to Eq. 6 a plot of log(|i_0|) versus T^{-1} should give a straight line.

$$\frac{\partial \log(i_0)}{\partial(1/T)} = -\frac{\Delta\overrightarrow{H}^{\ddagger}(E_{rev})}{R\ln(10)} \tag{6}$$

Such a plot is shown in Fig. 6, from the slope of the regression line given in the figure, and by the use of Eq. 6, the value of the activation enthalpy for cobalt deposition ($\Delta\overrightarrow{H}^{\ddagger}$) was 78 ± 18 Kj mol^{-1} for cobalt deposition. The error was estimated from the 95% confidence interval from the slope of the regression line. Plots of the current efficiency for cobalt deposition versus the current density for the four temperatures investigated, are given in Fig. 7, which shows that the current efficiency increases with increasing temperature. The reason for this effect was the fact that the overpotential for electrodeposition of cobalt was more dependent on the temperature than that of hydrogen evolution. From Fig. 7 it can be seen that the current efficiency for cobalt was higher at 40 °C than at 60 °C below about 200 A m^{-2}, contrary to the general trend. Therefore, it was suspected that this effect was due to experimental error, so both the experiments at 40 °C and 60 °C were repeated, showing the same trend. The reason for this anomaly was probably variations in the surface structure of cobalt during plating.

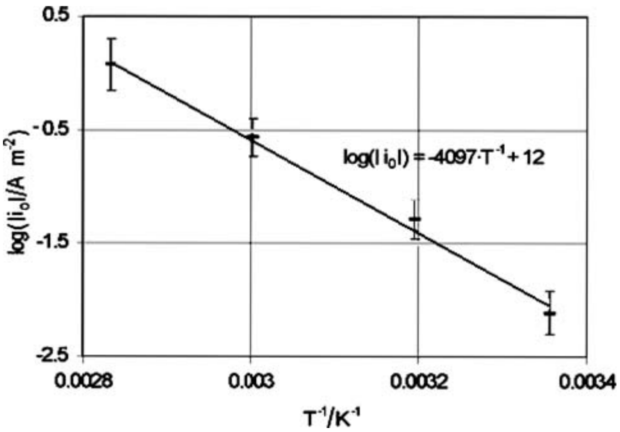

Fig. 6 Plot of log(|i_0|) versus T^{-1} for deposition of cobalt. The data points are given in Table 3

4 Conclusion

The current efficiency for cobalt deposition can be measured accurately on a rotating platinum disc electrode as the anodic charge for cobalt dissolution divided by the total cathodic charge. Current efficiencies for cobalt deposition increased with increasing current density and pH. In chloride electrolytes at pH between 1.08 and 2.08 the Tafel slope for cobalt deposition was –0.066 V decade^{-1} at 60 °C, indicating a pH independent reaction mechanism for electrodeposition of cobalt. In the pH range 3.0–4.4 the current for cobalt deposition increased with increasing pH at a given potential, indicating a pH dependent reaction mechanism. Increased temperature led to decreasing overpotential for cobalt electrodeposition and better current efficiency.

Table 3 Tafel parameters for deposition of cobalt at different temperatures

t/°C	E_{rev}/ V_{SHE}	b_c/V decade^{-1}	log(i_0/A m^{-2})	log(i/A m^{-2}) at –0.500 V_{SHE}	1–β
25	–0.290	–0.061 ± 0.003	–2.1 ± 0.2	1.32 ± 0.05	0.48 ± 0.02
40	–0.289	–0.064 ± 0.003	–1.3 ± 0.2	1.99 ± 0.04	0.48 ± 0.02
60	–0.288	–0.067 ± 0.004	–0.6 ± 0.2	2.56 ± 0.07	0.49 ± 0.03
80	–0.287	–0.071 ± 0.007	0.1 ± 0.2	3.0 ± 0.1	0.49 ± 0.05

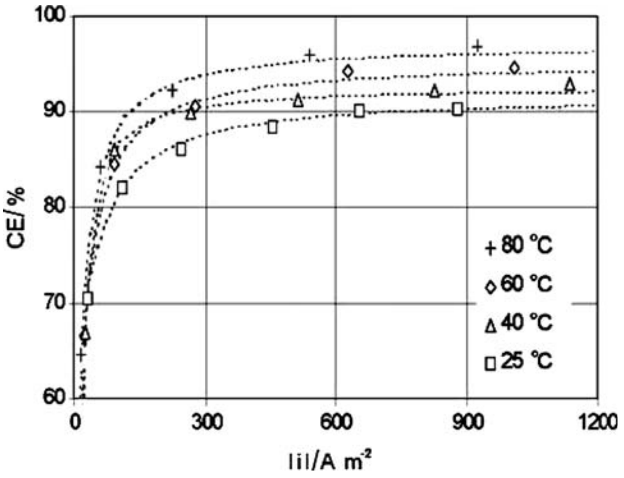

Fig. 7 Current efficiency for cobalt deposition versus current density at various temperatures

Acknowledgements Falconbridge Nikkelverk A/S in Norway and the Research Council of Norway (NFR) are acknowledged for financial support of this project.

References

1. Kerfoot DGE, Weir DR (1988) In: Tyroler GP, Landolt CA (eds) Extractive metallurgy of Nickel and Cobalt. The Metallurgical Society, Warrendale PA, pp 241–267
2. Fujimori M, Ono N, Tamura N, Kohga T (1982) In: Parker PD (ed) Chloride Electrometallurgy. The Metallurgical Society, Warrendale PA, pp 155–166
3. Stensholt EO, Zachariasen H, Lund JH (1986) Trans Inst Min Metall C95:C10
4. Grøntoft F (1980) Canadian Patent no. 1074251
5. Hultgren R, Desai PD, Hawkins DT, Gleiser M, Kelley KK (eds) (1973) Selected values of the properties of binary alloys. American Society for Metals, Metals Park, Ohio, pp 678–682
6. Meyer RJ (ed) Gmelins Handbuch der Anorganische Chemie, Co, Teil A. Verlag Chemie GmbH, Berlin, achte v̈ollige neu bearbeitete Auflag (1932)
7. Findlay T, Aylward G (1994) SI chemical data, 3rd edn. John Wiley & Sons, National Library of Australia
8. Scoyer J, Winand R (1977) Surf Technol 5:169
9. Louis P, Dille J, Hunga L, Shungu T (1988) In: Tyroler GP, Landolt CA (eds) Extractive metallurgy of Nickel and Cobalt. The Metallurgical Society, Warrendale PA, pp 505–515
10. Dille J, Charlier J, Winand R (1997) J Mater Sci 32:2637
11. Lenthall KC, Bryson AW (1997) In: Dreisinger DB (ed) Aqueous electrotechnology: progress in theory and practice. The Minerals, Metals & Materials Society, Warrendale PA, pp 305–320
12. Das SC, Subbaiah T (1984) Hydrometallurgy 12:317
13. Jeffrey MI, Choo WL, Breuer PL (2000) Miner Eng 13(12):1231
14. Feneau C, Breckpot R (1969) ATB: Metallurgie IX 3:115
15. Hausler KEZ (1962) Electrochem 66(2):177
16. Hausler KE (1967) Ber Bunsenges Phys Chem 71:620
17. Cui CQ, Jiang SP, Tseung ACC (1990) J Electrochem Soc 137(11):3418
18. Bolzan JA, Arvìa A (1962) J Electrochim Acta 7:589
19. Smith RM, Martell AE (1976) Critical stability constants. Plenum Press, New York